

**Reactions of Transition-Metal  $\sigma$ -Acetylide Complexes. 15.<sup>1</sup>**  
**Cycloaddition of**  
***trans*-1,2-Bis(methoxycarbonyl)-1-cyanoethene: Studies on the**  
**Mode of Ring Opening of  $\sigma$ -Cyclobutenyl Complexes. X-ray**  
**Structures of Two Isomers of**  
 **$\text{Ru}\{\text{C}=\text{CPhCH}(\text{CO}_2\text{Me})\text{C}(\text{CN})(\text{CO}_2\text{Me})\}\{\text{CO}\}(\text{PPh}_3)(\eta\text{-C}_5\text{H}_5)$ ,**  
 **$\text{Ru}\{\text{C}[\text{=C}(\text{CN})(\text{CO}_2\text{Me})]\text{CPh}=\text{CH}(\text{CO}_2\text{Me})\}\{\text{CO}\}(\text{PPh}_3)(\eta\text{-C}_5\text{H}_5)$ ,**  
**and  $\text{Ru}\{\eta^3\text{-CH}(\text{CO}_2\text{Me})\text{CPhC}=\text{C}(\text{CN})(\text{CO}_2\text{Me})\}\{\text{CO}\}(\eta\text{-C}_5\text{H}_5)$**

Michael I. Bruce,\* D. Neil Duffy, Michael J. Liddell, and Edward R. T. Tiekink

*Jordan Laboratories, Department of Physical and Inorganic Chemistry, University of Adelaide,  
Adelaide, South Australia 5001, Australia*

Brian K. Nicholson

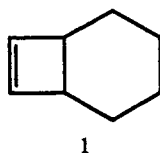
*School of Chemistry, University of Waikato, Hamilton, New Zealand*

Received May 31, 1991

Cycloaddition of *trans*-CH(CO<sub>2</sub>Me)=C(CN)(CO<sub>2</sub>Me) to Ru(C<sub>2</sub>Ph)(CO)(PPh<sub>3</sub>)( $\eta$ -C<sub>5</sub>H<sub>5</sub>) afforded two isomers of the cyclobutenyl complex Ru{C=CPhCH(CO<sub>2</sub>Me)C(CN)(CO<sub>2</sub>Me)}(CO)(PPh<sub>3</sub>)( $\eta$ -C<sub>5</sub>H<sub>5</sub>) (**5a,b**) formed by approach of the acetylide to each side of the olefin plane. Thermal opening of the cyclobutenyl ring occurred in conrotatory fashion in both complexes to give the same butadienyl, Ru{C[=C(CN)(CO<sub>2</sub>Me)]CPh=CH(CO<sub>2</sub>Me)}(CO)(PPh<sub>3</sub>)( $\eta$ -C<sub>5</sub>H<sub>5</sub>) (**6**); i.e., the  $\sigma$ -bonded transition-metal-ligand substituent does not affect the course of the reaction, which is in accord with the Woodward-Hoffmann rules. Further heating of the butadienyl complex resulted in loss of PPh<sub>3</sub> rather than CO and formation of Ru{ $\eta^3$ -CH(CO<sub>2</sub>Me)CPhC=C(CN)(CO<sub>2</sub>Me)}(CO)( $\eta$ -C<sub>5</sub>H<sub>5</sub>) (**9**). All four complexes were characterized by single-crystal X-ray studies: crystals of **5a** are monoclinic, space group *P*2<sub>1</sub>/*c*, with *a* = 14.719 (13) Å, *b* = 11.851 (6) Å, *c* = 18.572 (13) Å,  $\beta$  = 91.29 (4)°, *V* = 3238.8 Å<sup>3</sup>, and *Z* = 4; crystals of **5b** are orthorhombic, space group *Pna*2<sub>1</sub>, with *a* = 18.188 (7) Å, *b* = 18.059 (4) Å, *c* = 10.349 (5) Å, *V* = 3399.2 Å<sup>3</sup>, and *Z* = 4; crystals of **6** are triclinic, space group *P* $\bar{1}$ , with *a* = 9.227 (5) Å, *b* = 13.069 (9) Å, *c* = 15.860 (8) Å,  $\alpha$  = 98.44 (3)°,  $\beta$  = 92.17 (4)°,  $\gamma$  = 103.91 (3)°, *V* = 1831.0 Å<sup>3</sup>, and *Z* = 2; crystals of **9** are monoclinic, space group *P*2<sub>1</sub>/*n*, with *a* = 9.018 (3) Å, *b* = 12.244 (2) Å, *c* = 18.060 (4) Å,  $\beta$  = 104.56 (2)°, *V* = 1929.9 Å<sup>3</sup>, and *Z* = 4.

### Introduction

The stereochemical studies by Criegee et al.<sup>2</sup> on the thermal ring opening of *cis*- and *trans*-1,2,3,4-tetramethylcyclobutenes were the first to show unambiguously the conrotatory nature of the cyclobutene-butadiene electrocyclic interconversion. In contrast, 185-nm photolysis of hydrocarbon **1** yields *cis,cis*-1,3-cyclooctadiene



consistent with a disrotatory ring-opening mechanism.<sup>3</sup> In 1965, Woodward and Hoffmann<sup>4</sup> proposed a theory to rationalize such electrocyclic reactions. Since then, Brauman and Golden<sup>5</sup> have estimated that the thermally allowed conrotatory process for cyclobutenes is more fa-

vored (by 15.0 kcal/mol) than the disrotatory process. This experimental estimate is in accord with values obtained recently by Breulet and Schaefer<sup>6</sup> from ab initio calculations.

The torsional motion that is required to attain the transition state in electrocyclic reactions also plays a part in determining the direction of these reactions. Such motion has been found to be particularly crucial in cyclobutene complexes, where the products obtained from the ring-opening reactions are frequently in contrast to those expected from steric considerations. Rondan and Houk<sup>7</sup> have explained the results obtained in the electrocyclic reactions of perfluorocyclobutenes<sup>8</sup> and *cis* and *trans* 3,4-dichloro-, 3,4-dimethoxy-, 3,4-diethoxy-, and 3,4-diacetoxy-substituted cyclobutenes<sup>9</sup> as arising from the electronic effects of the cyclobutene substituents. Using ab initio calculations to determine transition-state structures, they established a preference for outward rotation in ring substituents with strong electron-donor capabilities, while  $\pi$ -acceptors such as ester and keto groups were shown to have little stereochemical preference.

(1) Part 14: Bruce, M. I.; Hambley, T. W.; Liddell, M. J.; Snow, M. R.; Swincer, A. G.; Tiekink, E. R. T. *Organometallics* 1990, 9, 96.

(2) (a) Criegee, R.; Noll, K. *Justus Liebigs Ann. Chem.* 1959, 672, 1. (b) *Chem. Ber.* 1965, 98, 2339.

(3) Clark, K. B.; Leigh, W. J. *J. Am. Chem. Soc.* 1987, 109, 6086.

(4) Woodward, R. B.; Hoffmann, R. *J. Am. Chem. Soc.* 1965, 87, 395, 2046, 2511, 4388.

(5) Brauman, J. I.; Golden, D. M. *J. Am. Chem. Soc.* 1968, 90, 1920.

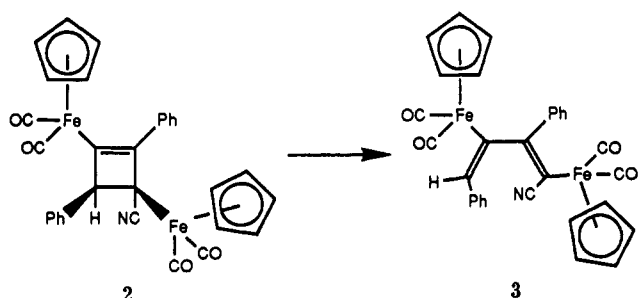
(6) Breulet, J.; Schaefer, H. F. *J. Am. Chem. Soc.* 1984, 106, 1221.

(7) Rondan, N. G.; Houk, K. N. *J. Am. Chem. Soc.* 1985, 107, 2099.

(8) Dolbier, W. R.; Koroniak, H.; Burton, D. J.; Heinze, P. L.; Bailey, A. R.; Shaw, G. S.; Hansen, S. W. *J. Am. Chem. Soc.* 1987, 109, 219 and references cited therein.

(9) Kirmse, W.; Rondan, N. G.; Houk, K. N. *J. Am. Chem. Soc.* 1984, 106, 7989.

Scheme I



Although the conversion of  $\sigma$ -cyclobutenyl to  $\sigma$ -butadienyl ligands has been reported on several occasions,<sup>1,10,11</sup> only one organometallic electrocyclic reaction has been described that allows the stereochemistry of the reaction to be discussed. This was the thermal conversion of the cyclobutenyldiiron complex  $\text{Fe}\{\text{C}(\text{C}=\text{CPh})\text{C}(\text{CN})\}[\text{Fe}(\text{CO})_2(\eta\text{-C}_5\text{H}_5)]\text{CHPh}$  (2) to the butadienyl complex  $\text{Fe}\{\text{C}(\text{C}=\text{CPh})\text{C}(\text{CN})\}[\text{Fe}(\text{CO})_2(\eta\text{-C}_5\text{H}_5)](\text{CO})_2(\eta\text{-C}_5\text{H}_5)$  (3) by Kolobova et al.<sup>12</sup> Although not mentioned in their report, their structural studies showed that the reaction had proceeded via the expected conrotatory process (Scheme I). As the frontier orbitals of transition-metal vinyl complexes (of which these cyclobutenyl and butadienyl complexes are examples) are likely to be involved in ring bonding,<sup>13</sup> the dimetal-substituted complexes might have electronic properties different from those of monometal-substituted complexes. We have therefore carried out further studies of the transformations of cycloadducts of transition-metal acetylides and activated olefins, using a substrate that has permitted the stereochemistry of the reactions to be determined.

## Results and Discussion

The availability of the olefin *trans*-1,2-bis(carbomethoxy)-1-cyanoethene [*trans*- $\text{C}(\text{CN})(\text{CO}_2\text{Me})=\text{CH}(\text{CO}_2\text{Me})$ , *rjo*]<sup>14</sup> has allowed us to examine its reactions with  $\text{Ru}(\text{C}_2\text{Ph})(\text{CO})(\text{PPh}_3)(\eta\text{-C}_5\text{H}_5)$  (4; Scheme II). Structural determinations of the products have permitted the direction of the ring-opening process to be determined and have also made possible direct comparisons with the cycloadducts obtained with  $\text{C}(\text{CF}_3)_2=\text{C}(\text{CN})_2$  (*dfe*).<sup>1,11</sup>

Three isomers of  $\text{Ru}\{\text{C}(\text{C}=\text{CPh})\text{CH}(\text{CO}_2\text{Me})\text{C}(\text{CN})(\text{CO}_2\text{Me})\}(\text{CO})(\text{PPh}_3)(\eta\text{-C}_5\text{H}_5)$ . Treatment of  $\text{Ru}(\text{C}_2\text{Ph})(\text{CO})(\text{PPh}_3)(\eta\text{-C}_5\text{H}_5)$  with *trans*- $\text{C}(\text{CN})(\text{CO}_2\text{Me})=\text{CH}(\text{CO}_2\text{Me})$  (*rjo*) in benzene resulted in the formation of two diastereoisomers of  $\text{Ru}\{\text{C}(\text{C}=\text{C}(\text{CN})(\text{CO}_2\text{Me})\text{C}(\text{CN})(\text{CO}_2\text{Me})\}(\text{CO})(\text{PPh}_3)(\eta\text{-C}_5\text{H}_5)$  (5a,b; Scheme II). The major isomer (59%) was 5a, which was separated readily from the minor isomer (27%) 5b by thin-layer chromatography. Proton NMR investigations of similar reactions performed in  $\text{CDCl}_3$  and  $\text{C}_6\text{D}_6$  showed that the reaction in  $\text{CDCl}_3$  was complete within 10 min, whereas that per-

formed in benzene took nearly 1.5 h. The ratio of isomers 5a/5b (2/1,  $\text{CDCl}_3$ ; 1.5/1,  $\text{C}_6\text{D}_6$ ) was only slightly altered by the differences in solvent polarity. No colored intermediates were detected in these reactions, and the ratio of isomers did not change after 7 days in solution ( $\text{CDCl}_3$ ).

It was noted that both isomers slowly changed color, from the pale yellow observed for 5b and white for 5a to a bright yellow when the isomers were supported on the silica TLC medium. A  $^1\text{H}$  NMR study of these reactions, performed on acetone-*d*<sub>6</sub> extracts of the supported samples, showed that when either of these complexes was adsorbed on silica, conversion to a third diastereoisomer (5c) occurred (Scheme III). The NMR results indicated that the conversion occurred only with adsorbed complexes in the solid state (dry), and control experiments with the NMR solvent and silica present did not reveal any formation of 5c. Maximum conversion of 5a to 5c was 58% after 50 h, while 5b was 25% converted after 14 days. Several side reactions were also noted, but of these only the conversions 5a  $\rightarrow$  5b and 5b  $\rightarrow$  5a could be correlated with the various  $\text{C}_5\text{H}_5$  and OMe resonances observed. A preparative-scale isomerization of 5a supported on silica allowed the isolation of 5c in 34% yield after 3 days. Suitable crystals of this complex could not be obtained for X-ray analysis, and it was characterized by microanalysis and spectroscopy alone.

The infrared data for all three cyclobutenyl complexes are similar. Very weak bands were observed between 2207 and 2236  $\text{cm}^{-1}$  for  $\nu(\text{CN})$  and between 1566 and 1616  $\text{cm}^{-1}$  for  $\nu(\text{C}=\text{C})$ . Single strong  $\nu(\text{CO})$  bands were found at ca. 1950  $\text{cm}^{-1}$  for the ruthenium-bond carbonyl and at ca. 1738  $\text{cm}^{-1}$  for the  $\text{CO}_2\text{Me}$  groups. The fingerprint region of 5c resembled more that of 5a than that of 5b.

In their proton NMR spectra,  $\text{C}_5\text{H}_5$ , CH, and two OMe resonances were observed for each complex at  $\delta$  5.14, 4.52, 3.74, 3.66 (5a),  $\delta$  4.91, 4.52, 3.85, 3.73 (5b), and  $\delta$  4.88, 4.18, 3.85, 3.51 (5c), respectively. The only unusual feature of these spectra was the apparent doublet at  $\delta$  4.52 ( $J = 1.6$  Hz) for the CH proton in the spectrum of 5b. Phosphorus coupling is ruled out by the behavior at low temperatures, the two resonances having relative intensities 1/1 at 298 K, changing to 4/3 at 240 K. Molecular modeling suggests that the minimum interaction between phenyl groups ( $\text{C}_2\text{Ph}$  and  $\text{PPh}_3$ ) may result from a structure in which there is restricted rotation of the CH-bound  $\text{CO}_2\text{Me}$  group. This in turn would result in two environments for the CH proton.

The FAB mass spectra of all three cyclobutenyl complexes were identical. A strong molecular ion, which fragmented by loss of Me, CO,  $\text{CO}_2\text{Me}$ , and  $\text{C}(\text{CN})(\text{CO}_2\text{Me})=\text{CH}(\text{CO}_2\text{Me})$  groups, was observed. The major ion is  $[\text{M} - \text{olefin}]^+$ , which is characteristic of cyclobutenyl complexes;<sup>10b</sup> it is not present in the mass spectrum of the related butadienyl complex  $\text{Ru}\{\text{C}(\text{C}=\text{C}(\text{CN})(\text{CO}_2\text{Me})\text{C}(\text{CN})(\text{CO}_2\text{Me})\}(\text{CO})(\text{PPh}_3)(\eta\text{-C}_5\text{H}_5)$  (6; see below). The other fragment ions present were associated with the loss of OMe,  $\text{CO}_2\text{Me}$ , and CO groups from the ions already mentioned or with the usual breakdown patterns observed for the  $\text{Ru}(\text{PPh}_3)(\eta\text{-C}_5\text{H}_5)$  group.

The molecular structures of 5a,b have been determined by single-crystal X-ray studies. Plots of the two molecules are shown in Figures 1 and 2, while Table I collects significant bond distances and angles. As mentioned above, 5a,b are diastereoisomers; one of the three asymmetric centers is the ruthenium atom.<sup>23</sup> Compound 5a crystallized in the centrosymmetric space group  $P2_1/c$ , whereas 5b crystallized in the noncentrosymmetric space group  $Pna2_1$ , implying that spontaneous resolution of the latter occurred during crystallization. About each ruthenium, the coor-

(10) (a) Bruce, M. I.; Hambley, T. W.; Snow, M. R.; Swincer, A. G. *Organometallics* 1985, 4, 494, 501. (b) Bruce, M. I.; Humphrey, P. A.; Snow, M. R.; Tiekink, E. R. T. *J. Organomet. Chem.* 1986, 303, 417. (c) Bruce, M. I.; Duffy, D. N.; Liddell, M. J.; Snow, M. R.; Tiekink, E. R. T. *J. Organomet. Chem.* 1987, 335, 365.

(11) Bruce, M. I.; Liddell, M. J.; Snow, M. R.; Tiekink, E. R. T. *Organometallics* 1988, 7, 343.

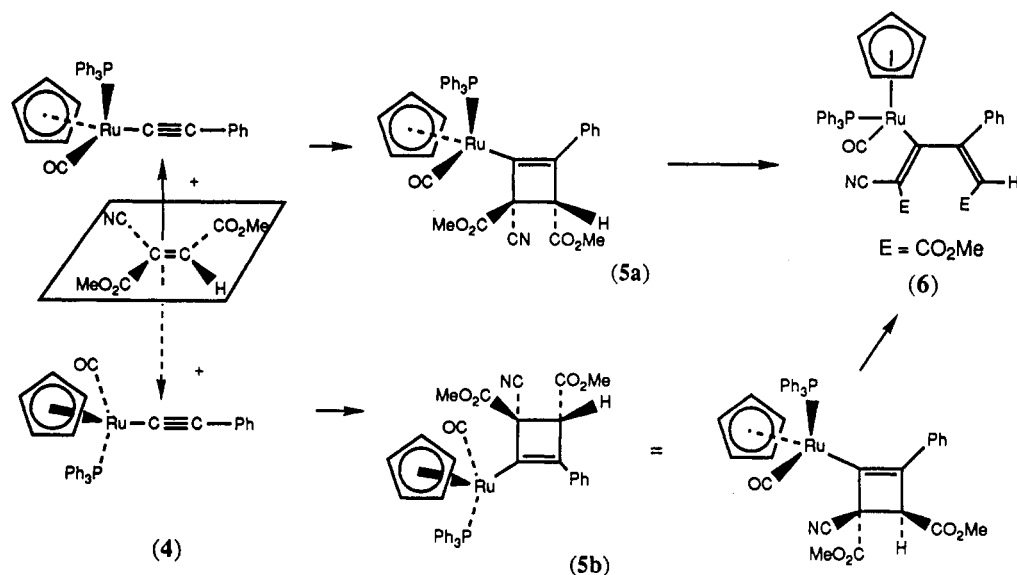
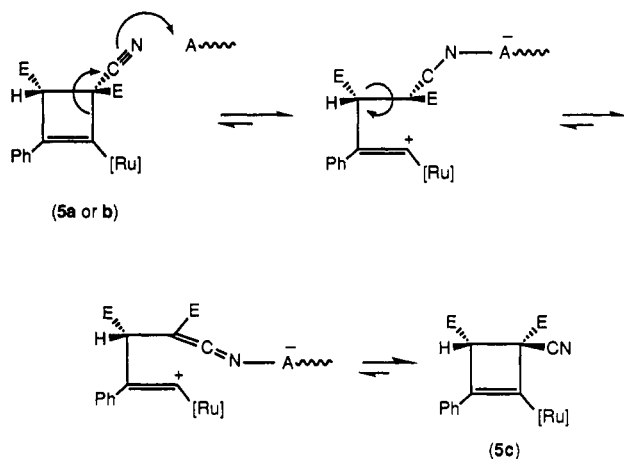
(12) Kolobova, N. E.; Rozantseva, T. V.; Struchkov, Yu. T.; Batsanov, A. S.; Bakhmutov, V. I. *J. Organomet. Chem.* 1985, 292, 247.

(13) Kostic, N. M.; Fenske, R. F. *Organometallics* 1982, 1, 974.

(14) Jackson, W. R.; Lovel, C. G. *Aust. J. Chem.* 1983, 36, 1975.

(15) (a) Bruce, M. I.; Catlow, A.; Humphrey, M. G.; Koutsantonis, G. A.; Snow, M. R.; Tiekink, E. R. T. *J. Organomet. Chem.* 1988, 338, 59. (b) Bruce, M. I.; Duffy, D. N.; Humphrey, M. G.; Swincer, A. G. *J. Organomet. Chem.* 1985, 282, 383.

Scheme II

Scheme III<sup>a</sup>

<sup>a</sup> Abbreviations: E = CO<sub>2</sub>Me; Ru = Ru(CO)(PPh<sub>3</sub>)( $\eta$ -C<sub>5</sub>H<sub>5</sub>).

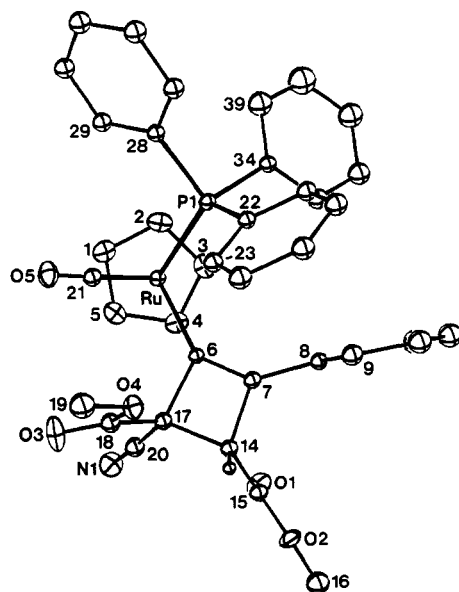


**Figure 1.** ORTEP view of a molecule of Ru[C=CPhCH-(CO<sub>2</sub>Me)C(CN)(CO<sub>2</sub>Me)](CO)(PPh<sub>3</sub>)( $\eta$ -C<sub>5</sub>H<sub>5</sub>) (5a), showing the atom-numbering scheme. Atoms not otherwise indicated are carbons.

Table I. Selected Interatomic Parameters for Complexes 5a,b, 6, and 9

	5a	5b	6	9 <sup>a</sup>
Distances (Å)				
Ru-P(1)	2.299 (1)	2.300 (2)	2.318 (2)	
Ru-C(6)	2.062 (5)	2.09 (1)	2.109 (6)	2.047 (4)
Ru-C(21)	1.831 (5)	1.81 (1)	1.833 (7)	1.875 (4)
Ru-cp	2.255- 2.276 (4)	2.233 (9)- 2.246 (8)	2.241- 2.273 (5)	2.227- 2.245 (3)
C(6)-C(7)	1.357 (7)	1.34 (2)	1.467 (8)	1.422 (5)
C(6)-C(17)	1.565 (7)	1.55 (1)	1.363 (8)	1.344 (5)
C(7)-C(8)	1.471 (6)	1.49 (1)	1.490 (7)	1.493 (4)
C(7)-C(14)	1.529 (7)	1.51 (1)	1.346 (9)	1.431 (5)
C(14)-C(15)	1.500 (7)	1.49 (2)	1.43 (2)	1.467 (5)
C(14)-C(17)	1.566 (4)	1.57 (2)		
C(17)-C(18)	1.529 (7)	1.51 (2)	1.479 (9)	1.483 (5)
C(17)-C(20)	1.477 (8)	1.48 (2)	1.44 (1)	1.443 (5)
C(20)-N(1)	1.137 (7)	1.12 (1)	1.140 (8)	1.137 (5)
C(21)-O(5)	1.160 (6)	1.19 (1)	1.168 (7)	1.145 (5)
Angles (deg)				
Ru-C(6)-C(7)	142.1 (4)	140.5 (8)	113.9 (4)	74.6 (2)
Ru-C(6)-C(17)	126.5 (3)	126.6 (7)	126.4 (7)	147.5 (3)
C(7)-C(6)-C(17)	90.9 (4)	91.1 (8)	118.8 (6)	136.5 (4)
C(6)-C(7)-C(14)	96.9 (4)	97.3 (9)	127.5 (6)	114.2 (3)
C(7)-C(14)-C(15)	111.8 (4)	124.3 (9)	127.8 (7)	121.4 (3)
C(7)-C(14)-C(17)	84.8 (4)	84.7 (8)		
C(15)-C(14)-C(17)	117.7 (4)	116.2 (9)		
C(6)-C(17)-C(14)	87.4 (3)	86.9 (7)		
C(6)-C(17)-C(18)	115.0 (4)	112.6 (9)	122.3 (6)	125.5 (4)
C(6)-C(17)-C(20)	115.3 (4)	115.1 (8)	124.5 (2)	121.7 (4)
C(14)-C(17)-C(18)	115.6 (4)	112 (1)		
C(14)-C(17)-C(20)	117.2 (4)	114.9 (9)		
C(18)-C(17)-C(20)	106.1 (4)	113.2 (9)	113.1 (6)	112.5 (3)

<sup>a</sup> Ru-C(7) = 2.160 (4) Å; Ru-C(14) = 2.218 (4) Å; Ru-C(7)-C(6) = 66.0 (2)°; Ru-C(14)-C(7) = 68.7 (2)°.

dination is distorted octahedral, with one face occupied by the  $\eta$ -C<sub>5</sub>H<sub>5</sub> group and the other face defined by the carbonyl, triphenylphosphine, and  $\sigma$ -cyclobutenyl ligands. The ligand-ruthenium bond distances in complexes 5a,b (Ru-C(21) = 1.831 (5), 1.81 (1) Å, respectively; Ru-P(1) = 2.299 (1), 2.300 (2) Å, respectively; Ru-C(cp) = 2.255 (4)-2.267 (4), 2.233 (9)-2.246 (8) Å, respectively; are similar to those found for other Ru(CO)(PPh<sub>3</sub>)( $\eta$ -C<sub>5</sub>H<sub>5</sub>) compounds,<sup>16</sup> the differences between the two structures being within the range of experimental error. The Ru-C(sp<sup>2</sup>)

(16) (a) Garrett, K. E.; Sheridan, J. B.; Pourreau, D. B.; Feng, W. C.; Geoffroy, G. L.; Staley, D. L.; Rheingold, A. L. *J. Am. Chem. Soc.* 1989, 111, 8383. (b) Brisdon, B. J.; Deeth, R. J.; Hodson, A. G. W.; Kemp, C. M.; Mahon, M. F.; Malloy, K. C. *Organometallics* 1991, 10, 1107.

(17) Bruce, M. I.; Wallis, R. C. *Aust. J. Chem.* 1979, 32, 1471. Bruce, M. I.; Swincer, A. G. *Aust. J. Chem.* 1980, 33, 1471.

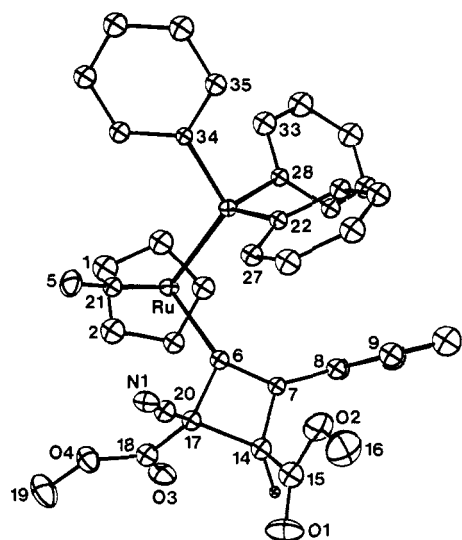
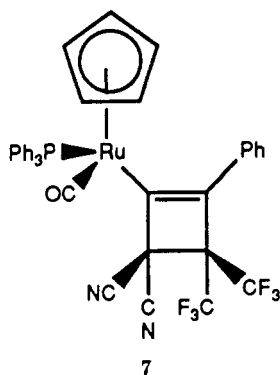


**Figure 2.** ORTEP view of a molecule of  $\text{Ru}\{\text{C}=\text{CPhCH}(\text{CO}_2\text{Me})\text{C}(\text{CN})(\text{CO}_2\text{Me})\}(\text{CO})(\text{PPh}_3)(\eta\text{-C}_5\text{H}_5)$  (**5b**), showing the atom-numbering scheme. Atoms not otherwise indicated are carbons.

distances (2.062 (5) (**5a**) and 2.09 (1) Å (**5b**)) are similar to that observed for  $\text{Ru}\{\text{C}=\text{CPhC}(\text{CF}_3)_2\text{C}(\text{CN})_2\}(\text{CO})(\text{PPh}_3)(\eta\text{-C}_5\text{H}_5)$  (**7**) (2.054 (8) Å).<sup>1</sup> Within the  $\text{C}_4$  ring the



pattern of bond lengths for **5a,b** ( $\text{C}(6)\text{--}\text{C}(7) = 1.357$  (7), 1.34 (2) Å, respectively;  $\text{C}(7)\text{--}\text{C}(14) = 1.529$  (7), 1.51 (1) Å, respectively;  $\text{C}(14)\text{--}\text{C}(17) = 1.566$  (4), 1.57 (2) Å, respectively;  $\text{C}(17)\text{--}\text{C}(6) = 1.565$  (7), 1.55 (1) Å, respectively; is similar to that found for **7**,<sup>1</sup> with perhaps the only difference being the slight contraction of the single bond closest to the ruthenium ( $\text{C}(17)\text{--}\text{C}(6)$ ; cf. 1.57 (1) Å in **7**). The angles subtended at the  $\text{sp}^2$  carbon atoms range from 90.9 (4) to 97.3 (9)° and, at the  $\text{sp}^3$  carbon atoms, from 84.7 (8) to 87.4 (3)°. All of these fall within the normal range found for the cyclobutenyl complexes examined so far.<sup>1,10,11</sup> The cyclobutenyl rings in the two structures are essentially planar, the ruthenium atom lying 0.222 Å below the least-squares plane through the ring carbons in **5a** and 0.364 Å below the same plane in **5b**.

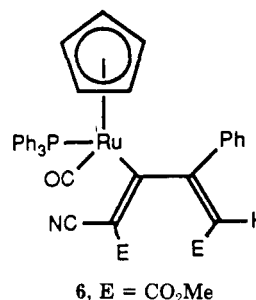
The difference between the isomers is most clearly seen when one examines the disposition of the CN group. In **5a**, the CN group attached to  $\text{C}(17)$  is on the same side of the ring as the ruthenium. In **5b**, the CN group is on the other side of the ring. This suggests that the preferred direction of addition of the  $=\text{C}(\text{CN})(\text{CO}_2\text{Me})$  group of the olefin is toward the  $\alpha$ -carbon of the acetylide, with  $\text{CO}_2\text{Me}$  in the least sterically demanding position. Clearly, the CN group is directing the initial attack of the olefin on the acetylide, as neither of the other isomers formed by the reverse addition of the olefin was observed. This is con-

sistent with previous work with  $\text{dcfe}^{1,11}$  and ortho-substituted styrenes.<sup>10b</sup> The similarity with the results obtained with  $\text{tcne}^{10a}$  points again to the involvement of a dipolar intermediate, which converts quickly to the cyclobutenyl complexes on account of the high degree of polarizability inherent in the present olefin; the  $\text{C}(\text{CN})(\text{CO}_2\text{Me})$  group efficiently stabilizes the negative charge. The two isomers are formed by approach of the acetylide complex above and below the plane of the olefin (Scheme II).

The structure of the third cyclobutenyl isomer was investigated by means of molecular modeling (CHEM 3D). It appears that no minor orientational forms due to restricted rotation are available, as the only appreciable interactions are between phenyl groups and these are most likely to affect crystal packing. On the basis of similarities in the phenyl regions of the  $^1\text{H}$  NMR spectra and the fingerprint regions of the IR spectra, we suggest a structure related to isomer **5a** by rotation of the  $\text{CO}_2\text{Me}$  group on  $\text{C}(14)$  to the side of the ring opposite to the ruthenium. This places both  $\text{CO}_2\text{Me}$  groups on the same side of the ring.

Maximum interaction between the oxygen atoms of the  $\text{CO}_2\text{Me}$  and CO groups with the surface siloxy groups of the silica, and minimum contact between the phenyl and cyclopentadienyl groups and the surface, is achieved for **5c** when the base of the ring is in contact with the surface region. As **5c** is recovered from the surface by extraction with methanol/ $\text{CH}_2\text{Cl}_2$  mixtures, only adsorption seems to be involved. The transformation from **5a** to **5b** and vice versa on silica indicates that significant rearrangements of the substituents on the ring are possible. The intermediate involved in these transformations could be **5c**. The formation of **5c** shows that bond-breaking processes have occurred. At present we are inclined to favor the breaking of  $\text{C}(6)\text{--}\text{C}(17)$ , followed by rotation about  $\text{C}(14)\text{--}\text{C}(17)$  and then ring closure rather than formation of a butadiene followed by recyclization. These reactions are probably Lewis-acid-catalyzed by silica surface sites, denoted A in Scheme III.

**Conrotatory Ring Opening.** Pyrolysis of both isomers **5a,b** resulted in the formation of the same complex, the butadienyl compound **6**. The reaction of **4** with  $\text{rjo}$ , followed by heating the crude reaction product (a mixture of **5a,b**) for 16 h in benzene (80 °C), gave yellow crystalline **6** directly in 60% yield.



In the IR spectrum of **6**, a weak  $\nu(\text{CN})$  band was observed at 2207  $\text{cm}^{-1}$  and strong  $\nu(\text{CO})$  absorptions were found at 1951 and 1725  $\text{cm}^{-1}$  for the ruthenium-bound carbonyl and the ester carbonyls, respectively. The  $\nu(\text{C}=\text{C})$  absorptions at 1597–1501  $\text{cm}^{-1}$  had intensities varying from very weak to strong. The proton NMR spectrum contained resonances for the CH,  $\text{C}_5\text{H}_5$ , and two  $\text{CO}_2\text{Me}$  groups at  $\delta$  5.41, 4.74, 3.58, and 3.14, respectively. In the FAB mass spectrum of **6**, a strong molecular ion, which fragmented by loss of Me, CO, and  $\text{C}_5\text{H}_5$  groups, was observed. An interesting difference between **6** and the isomers of **5** was the loss of the  $\text{C}_5\text{H}_5$  group. No loss of the

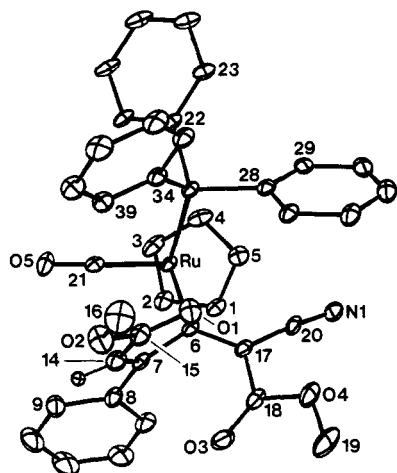
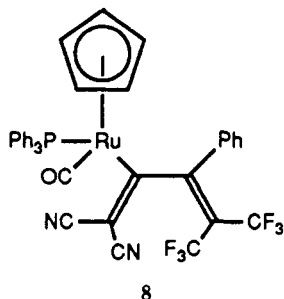


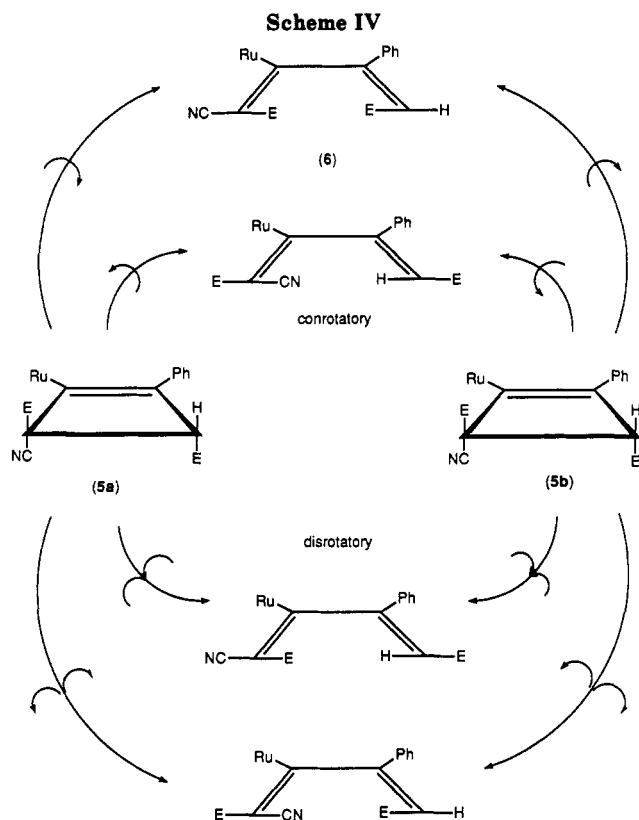
**Figure 3.** ORTEP view of a molecule of  $\text{Ru}\{\text{C}[\text{=C}(\text{CN})\text{-(CO}_2\text{Me)]CPh=CH(CO}_2\text{Me)}\}(\text{CO})(\text{PPh}_3)(\eta\text{-C}_5\text{H}_5)$  (6), showing the atom-numbering scheme. Atoms not otherwise indicated are carbons.

olefin from the molecular ion occurred, suggesting the butadienyl structure shown by an X-ray crystal structure determination.

A plot of one molecule of 6 is shown in Figure 3, and significant bond distances and angles are collected in Table I. As with 5, there is an asymmetric center at ruthenium; in the crystal both enantiomers are present. The absolute configuration of the molecule illustrated in Figure 3 is *S*. The ruthenium is coordinated to the carbonyl, triphenylphosphine, and  $\eta\text{-C}_5\text{H}_5$  ligands in a fashion similar to that found in 5a,b. The distances Ru-C(21) (1.833 (7) Å), Ru-P (2.318 (2) Å), and Ru-C(cp) (2.241–2.273 (5) Å) are also comparable. The orientation of the butadienyl ligand is very similar to that observed in  $\text{Ru}\{\text{C}[\text{=C}(\text{CN})_2]\text{CPh}=\text{C}(\text{CF}_3)_2\}(\text{CO})(\text{PPh}_3)(\eta\text{-C}_5\text{H}_5)$  (8),<sup>1</sup> as are the Ru-C(sp<sup>2</sup>) (2.109 (6) Å), C=C (1.346 (9), 1.363 (8) Å), and C-C (1.469 (8) Å) bond distances (cf. respectively 2.100 (5); 1.356 (7), 1.367 (7); 1.480 (7) Å in 8).



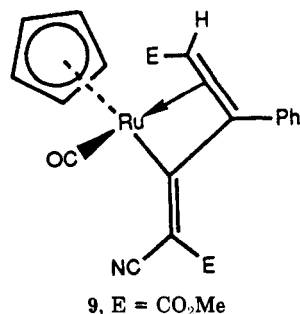
The use of modeling has shown that the cyclobutenyl rings in both isomers open in a conrotatory fashion, which is as predicted by the principles of conservation of orbital symmetry developed by Woodward and Hoffmann.<sup>4</sup> Scheme IV depicts the two transformations and, for completeness' sake, the disrotatory processes which would result in the observed butadienyl complex (complex 6 would not be obtained in a disrotatory fashion from either 5a or 5b). Isomer 5c is one of the cyclobutenyl complexes which should form 6 by a disrotatory mechanism; unfortunately, we were not able to determine the nature of the product formed by ring opening of 5c. This isomer does not appear to be involved in the formation of 6 from 5a,b, since no interconversion was found between 5a, 5b, and 5c in solution. It is interesting to note that in these electrocyclic reactions the CO<sub>2</sub>Me substituents on C(14) and C(17) both rotate inward as the ring opens, which



might be expected to lead to maximum steric interaction between these substituents. This result is in accord with recent transition-state calculations for organic cyclobutenes; these indicated that ester groups show little preference for either inward or outward rotation while cyano groups show a preference for outward rotation.<sup>9</sup>

In the course of the ring opening, the butadiene rotates about the Ru-C(6) bond and internally about the C(6)-C(7) bond to achieve the structure that is observed in the solid state. The coplanar diene structure is not favored because of the overlap between the CO<sub>2</sub>Me groups, rotation about C(6)-C(7) being necessary to relieve these interactions. This in turn creates phenyl-phenyl interactions that are minimized by rotation about the Ru-C(6) bond. The torsion angle C(14)C(7)C(6)C(17) is 97.2°, reflecting these effects. An interesting feature of most of the butadienyl complexes studied is the relative constancy of this torsion angle.

**Allyl Complex  $\text{Ru}\{\eta^3\text{-CH}(\text{CO}_2\text{Me})\text{CPhC}=\text{C}(\text{CN})\text{-(CO}_2\text{Me)}\}(\text{CO})(\eta\text{-C}_5\text{H}_5)$  (9).** A minor product from the pyrolyses of 5a,b was  $\text{Ru}\{\eta^3\text{-CH}(\text{CO}_2\text{Me})\text{CPhC}=\text{C}(\text{CN})\text{-(CO}_2\text{Me)}\}(\text{CO})(\eta\text{-C}_5\text{H}_5)$  (9). Higher yields of this complex were obtained by increasing the duration or temperature of the pyrolyses. A 57% yield of 9 was obtained after heating 5a in refluxing xylene for 24.5 h and a 38% yield from 5b after heating in refluxing toluene for 29 h.



9, E = CO<sub>2</sub>Me

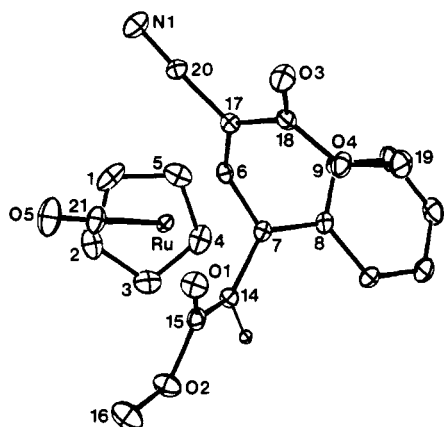
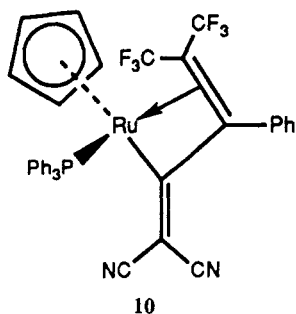


**Figure 4.** ORTEP view of a molecule of  $\text{Ru}\{\eta^3\text{-C}[\text{=C}(\text{CN})\text{-(CO}_2\text{Me)]CPh=CH(CO}_2\text{Me)}\}(\text{CO})(\eta^5\text{-C}_5\text{H}_5)$  (**9**), showing the atom-numbering scheme. Atoms not otherwise indicated are carbons.

The IR spectrum of **9** has a weak  $\nu(\text{CN})$  absorption at  $2220\text{ cm}^{-1}$  and a medium-intensity  $\nu(\text{C}=\text{C})$  band at  $1647\text{ cm}^{-1}$ . An increase in the energy of the  $\nu(\text{CO})$  band of the ruthenium-bound carbonyl to  $2014\text{ cm}^{-1}$  was found and suggests that the metal has a lower electron density than in **5a,b** and **6**, consistent with the loss of  $\text{PPh}_3$ . The ester carbonyl absorptions were found at  $1736$ ,  $1715$ , and  $1665\text{ cm}^{-1}$ .

Comparison of the relative intensities of the phenyl ( $\delta$  7.3–7.2) and cyclopentadienyl ( $\delta$  5.04) resonances in the proton NMR spectrum confirmed loss of  $\text{PPh}_3$  in the formation of **9** from **5**. Three other resonances were found at  $\delta$  5.09, 3.66, and 3.55 for the CH and the two  $\text{CO}_2\text{Me}$  groups, respectively. In the FAB mass spectrum, a strong molecular ion was found, but higher mass aggregates were also observed at  $m/z$  930, 902, 630, and 602; these correspond to  $[\text{M}_2]^+$ ,  $[\text{M}_2 - \text{CO}]^+$ ,  $[\text{M} + \text{Ru}(\text{C}_5\text{H}_5)]^+$ , and  $[\text{M} - \text{CO} + \text{Ru}(\text{C}_5\text{H}_5)]^+$ . The relative intensities of these aggregate ions were less than 5%, and closer examination of the spectra of related allyl complexes revealed similar weak binuclear ions. The major fragment ions correspond to loss of CO and Me groups, followed by the loss of both  $\text{CO}_2\text{Me}$  groups.

A plot of the structure of **9** determined by X-ray crystallography is shown in Figure 4, and significant bond distances and angles are collected in Table I. The  $\eta^5\text{-C}_5\text{H}_5$  and CO ligands are arranged about the ruthenium in a fashion similar to that observed for the dcfe-derived allyl complex  $\text{Ru}\{\eta^3\text{-C}(\text{CF}_3)_2\text{CPh}=\text{C}(\text{CN})_2\}(\text{PPh}_3)(\eta^5\text{-C}_5\text{H}_5)$  (**10**),<sup>1</sup> except that the CO group occupies the  $\text{PPh}_3$  site.



The bond distances for Ru–C(21) ( $1.875(4)\text{ \AA}$ ) and Ru–C(cp) ( $2.227\text{--}2.245(3)$ , average  $2.236\text{ \AA}$ ) are within their normal ranges. The Ru–C(21) distance is slightly longer (ca.  $0.04\text{ \AA}$ ) than those observed for **5a,b** and **6** ( $1.831(5)$ ,  $1.81(1)$ ,  $1.833(7)\text{ \AA}$ , respectively).

The allyl group is attached to the ruthenium in the same manner as observed for complex **10** mentioned above. The

shortest bond is Ru–C(6) ( $2.047(4)\text{ \AA}$ ; cf.  $1.977(7)\text{ \AA}$  in **10**); Ru–C(7) and Ru–C(14) are longer ( $2.160(4)$ ,  $2.218(4)\text{ \AA}$ , respectively; cf.  $2.138(7)$ ,  $2.202(7)\text{ \AA}$ , respectively, in **10**). The distances within the allyl ligand C(6)–C(7) and C(7)–C(14) ( $1.422(5)$ ,  $1.431(5)\text{ \AA}$ , respectively; cf.  $1.42(1)$ ,  $1.46(1)\text{ \AA}$ , respectively, in **10**) are normal allyl C–C separations indicative of multiple-bond order, while C(6)–C(17) ( $1.344(5)\text{ \AA}$ ; cf.  $1.37(1)\text{ \AA}$  in **10**) is a typical C=C double-bond length. The reduction in Ru–C multiple bonding in the rjo-derived allyl **9**, compared with that in the other related structurally characterized allyl complexes, may arise from the absence of the  $\text{PPh}_3$  (a good  $\sigma$ -donor) from the ruthenium. Formulation as a vinylcarbene complex<sup>16a</sup> or as an  $\eta^3(4e)$ -butadienyl species is also consistent with the structural data. After completion of this work, a theoretical study of related molybdenum complexes supported the latter interpretation.<sup>16b</sup>

It is clear from the reaction conditions that the allyl complex **9** is formed from the butadienyl compound **6**. Modeling the interconversion has shown that the phenyl and  $=\text{C}(\text{CN})(\text{CO}_2\text{Me})$  groups interact strongly with the triphenylphosphine when the butadienyl is rotated about the Ru–C(6) bond. It is probably this interaction that is responsible for the loss of the larger triphenylphosphine ligand rather than the CO group. The orientation of the allyl group is related to that of the butadienyl precursor by a rotation about Ru–C(6). Torsion angles about RuC(6)C(7)C(14) and RuC(7)C(6)C(17) in **6** and **9** are  $-107.22$ ,  $-169.97^\circ$  and  $-56.91$ ,  $168.77^\circ$ , respectively.

**Conclusions.** The  $[2 + 2]$  cycloaddition of the unsymmetrical olefin rjo to  $\text{Ru}(\text{C}_2\text{Ph})(\text{CO})(\text{PPh}_3)(\eta^5\text{-C}_5\text{H}_5)$  gave two isomers of a cyclobutenyl complex, **5a,b**, which differ in the position of the trans- $\text{CO}_2\text{Me}$  groups with respect to the metal core. When they were supported on silica, complexes **5a,b** isomerized to a third cyclobutenyl complex, **5c**. The thermal ring-opening reactions of both **5a** and **5b** proceeded in the conrotatory direction predicted by Woodward–Hoffmann rules to give the same butadienyl complex **6**. Further pyrolysis of **6** gave the vinylcarbene complex **9**, which was formed by unexpected loss of a  $\text{PPh}_3$  ligand.

## Experimental Section

**General Conditions.** General conditions and instrumentation were as given previously.<sup>1</sup>

**Starting Materials.** The literature method was used to prepare  $\text{Ru}(\text{C}_2\text{Ph})(\text{CO})(\text{PPh}_3)(\eta^5\text{-C}_5\text{H}_5)$ ;<sup>18</sup> *trans*- $\text{CH}(\text{CO}_2\text{Me})=\text{C}(\text{CN})(\text{CO}_2\text{Me})$  was generously provided by Professor W. R. Jackson (Monash University).<sup>14</sup>

Molecular modeling was performed using the CHEM 3D program for Apple Macintosh computers supplied by Cambridge Scientific Computing (1987). The covalent radii and bond distances and angles were those found in the CHEM 3D parameter set, modified where necessary by values obtained from the crystallographic studies.

**Synthesis of Two Isomers of  $\text{Ru}\{\text{C}=\text{CPhCH}(\text{CO}_2\text{Me})\text{C}(\text{CN})(\text{CO}_2\text{Me})\}(\text{CO})(\text{PPh}_3)(\eta^5\text{-C}_5\text{H}_5)$  (**5a,b**).** (a) The olefin  $\text{C}(\text{CN})(\text{CO}_2\text{Me})=\text{CH}(\text{CO}_2\text{Me})$  ( $69\text{ mg}$ ,  $0.41\text{ mmol}$ ) was added to a solution of  $\text{Ru}(\text{C}_2\text{Ph})(\text{CO})(\text{PPh}_3)(\eta^5\text{-C}_5\text{H}_5)$  ( $200\text{ mg}$ ,  $0.36\text{ mmol}$ ) in  $\text{CH}_2\text{Cl}_2$  ( $10\text{ mL}$ ). After 17 h the solvent was removed under reduced pressure. Preparative TLC of the residue (petroleum ether/acetone/ $\text{CH}_2\text{Cl}_2$  7/3/1) isolated two major bands. The first off-white band ( $R_f$  0.69) was collected and crystallized ( $\text{CH}_2\text{Cl}_2/\text{MeOH}$ ) to give white crystals of  $\text{Ru}\{\text{C}=\text{CPhCH}(\text{CO}_2\text{Me})\text{C}(\text{CN})(\text{CO}_2\text{Me})\}(\text{CO})(\text{PPh}_3)(\eta^5\text{-C}_5\text{H}_5)\cdot 0.25\text{CH}_2\text{Cl}_2$  (**5a**;  $160\text{ mg}$ ,  $0.21\text{ mmol}$ ,  $59\%$ ), mp  $181\text{--}182^\circ\text{C}$ . Anal. Calcd for  $\text{C}_{39}\text{H}_{32}\text{N}_6\text{O}_5\text{PRu}\cdot 0.25\text{CH}_2\text{Cl}_2$ : C, 63.04; H, 4.35; N, 1.87;  $M_r$ , 727

(18) ABSORB: Absorption Correction Programme for CAD4 Diffractometer; University of Sydney: Sydney, Australia, 1980.

(unsolvated). Found: C, 63.08; H, 4.31; N, 1.87;  $M_r$ , 727 (mass spectrometry). IR ( $\text{CH}_2\text{Cl}_2$ ;  $\text{cm}^{-1}$ ):  $\nu(\text{CN})$  2236 (vw);  $\nu(\text{CO})$  1950 (vs), 1738 (s).  $^1\text{H NMR}$  ( $\text{CDCl}_3$ ;  $\delta$ ): 7.4–6.5 (m, 20 H, Ph); 5.30 (s, 0.5 H,  $\text{CH}_2\text{Cl}_2$ ); 5.14 (s, 5 H,  $\text{C}_5\text{H}_5$ ); 4.52 (s, 1 H, CH); 3.74 (s, 3 H,  $\text{CO}_2\text{Me}$ ); 3.66 (s, 3 H,  $\text{CO}_2\text{Me}$ ). FAB MS ( $m/z$ ): 717\*,  $[\text{M}]^+$ , 24; 712\*,  $[\text{M} - \text{Me}]^+$ , 1; 698\*,  $[\text{M} - \text{CO}]^+$ , 5; 668\*,  $[\text{M} - \text{CO}_2\text{Me}]^+$ , 3; 637\*,  $[\text{M} - \text{OMe}]^+$ , 2; 621\*,  $[\text{M} - \text{O}_2\text{Me}]^+$ , 4; 558,  $[\text{M} - \text{C}(\text{CN})(\text{CO}_2\text{Me})=\text{CH}(\text{CO}_2\text{Me})]^+$ , 85; 529\*,  $[\text{M} - \text{CO}]^+$ , 9; 457\*,  $[\text{Ru}(\text{CO})(\text{PPh}_3)(\text{C}_5\text{H}_5)]^+$ , 30; 429\*,  $[\text{Ru}(\text{PPh}_3)(\text{C}_5\text{H}_5)]^+$ , 100; 378\*,  $[\text{Ru}(\text{CO})(\text{PPh}_2)(\text{C}_5\text{H}_5)]^+$ , 9; 362\*,  $[\text{Ru}(\text{PPh}_3)]^+$ , 13; 352\*,  $[\text{Ru}(\text{PPh}_2)(\text{C}_5\text{H}_5)]^+$ , 20; 285\*,  $[\text{Ru}(\text{PPh}_2)]^+$ , 9; 244,  $[\text{RuPh}(\text{C}_5\text{H}_5)]^+$ , 13; 167,  $[\text{Ru}(\text{C}_5\text{H}_5)]^+$ , 13.

The second pale yellow band ( $R_f$  0.61) crystallized ( $\text{CH}_2\text{Cl}_2/\text{MeOH}$ ) as yellow crystals of  $\text{Ru}\{\text{C}=\text{CPhCH}(\text{CO}_2\text{Me})\text{C}(\text{CN})(\text{CO}_2\text{Me})\}(\text{CO})(\text{PPh}_3)(\eta\text{-C}_5\text{H}_5)$  (**5b**; 83 mg, 0.11 mmol, 27%), mp 181–182 °C. Anal. Calcd for  $\text{C}_{39}\text{H}_{32}\text{NO}_5\text{PRu}$ : C, 64.46; H, 4.44; N, 1.91;  $M_r$ , 727. Found: C, 63.96; H, 4.59; N, 1.93;  $M_r$ , 727 (mass spectrometry). IR ( $\text{CH}_2\text{Cl}_2$ ;  $\text{cm}^{-1}$ ):  $\nu(\text{CN})$  2236 (vw);  $\nu(\text{CO})$  1958 (vs), 1738 (s).  $^1\text{H NMR}$  ( $\text{CDCl}_3$ ;  $\delta$ ): 7.4–6.8 (m, 20 H, Ph); 4.91 (s, 5 H,  $\text{C}_5\text{H}_5$ ); 4.52 (d,  $J_{\text{PH}} = 1.6$  Hz, 1 H, CH); 3.85 (s, 3 H,  $\text{CO}_2\text{Me}$ ); 3.73 (s, 3 H,  $\text{CO}_2\text{Me}$ ). FAB MS: identical in observed peaks and intensities with those of **5a**. A trace red band and six trace white bands were observed but not identified.

(b) For the  $^1\text{H NMR}$  study of the formation of **5a** and **5b**,  $\text{Ru}(\text{C}_2\text{Ph})(\text{CO})(\text{PPh}_3)(\eta\text{-C}_5\text{H}_5)$  (15 mg, 0.027 mmol) dissolved in  $\text{CDCl}_3$  (0.5 mL) was added to  $\text{C}(\text{CN})(\text{CO}_2\text{Me})=\text{CH}(\text{CO}_2\text{Me})$  (5 mg, 0.03 mmol) and then placed in an NMR tube. After 4 min only a trace of acetylide was found to be present and within 10 min the formation of **5a,b** was complete. The equilibrium ratio of isomers **5a/5b** (2.0/1) was the same after 7 days in solution. When a similar experiment was performed using  $\text{C}_6\text{D}_6$ , the equilibrium ratio was 1.5/1 after a reaction time of 85 min.

**Solid-State Conversion of 5a and 5b to a Third Isomer of  $\text{Ru}\{\text{C}=\text{CPhCH}(\text{CO}_2\text{Me})\text{C}(\text{CN})(\text{CO}_2\text{Me})\}(\text{CO})(\text{PPh}_3)(\eta\text{-C}_5\text{H}_5)$  (**5c**).** (a) **Conversion of 5a to 5c.** Isomer **5a** (65 mg, 0.09 mmol) was dissolved in  $\text{CH}_2\text{Cl}_2$  (10 mL), silica (TLC grade; 800 mg) was added, and the solvent was removed. After 3 days in the dark, exposed to air, the silica had become yellow. Following solvent extraction ( $\text{CH}_2\text{Cl}_2/\text{MeOH}$ ) the residue was separated by TLC (petroleum ether/ $\text{CH}_2\text{Cl}_2$ /acetone 4/2/1). Two bands were collected: the first white band ( $R_f$  0.53) was identified ( $^1\text{H NMR}$ , spot TLC) as recovered **5a** (16 mg, 24%); the next yellow band ( $R_f$  0.44) crystallized ( $\text{CH}_2\text{Cl}_2$ /petroleum ether) as pale yellow crystals of  $\text{Ru}\{\text{C}=\text{CPhCH}(\text{CO}_2\text{Me})\text{C}(\text{CN})(\text{CO}_2\text{Me})\}(\text{CO})(\text{PPh}_3)(\eta\text{-C}_5\text{H}_5)$  (**5c**; 22 mg, 0.03 mmol, 34%), mp 177–179 °C. Anal. Calcd for  $\text{C}_{39}\text{H}_{32}\text{NO}_5\text{PRu}\cdot 0.1\text{CH}_2\text{Cl}_2$ : C, 63.88; H, 4.41; N, 1.91;  $M_r$ , 727 (unsolvated). Found: C, 63.83; H, 4.40; N, 1.92;  $M_r$ , 727 (mass spectrometry). IR ( $\text{CH}_2\text{Cl}_2$ ;  $\text{cm}^{-1}$ ):  $\nu(\text{CN})$  2235 (vw), 2207 (vw);  $\nu(\text{CO})$  1953 (vs), 1737 (s).  $^1\text{H NMR}$  ( $\text{CDCl}_3$ ;  $\delta$ ): 7.4–6.6 (m, 20 H, Ph); 5.30 (s, 0.2 H,  $\text{CH}_2\text{Cl}_2$ ); 4.88 (s, 5 H,  $\text{C}_5\text{H}_5$ ); 4.18 (s, 1 H, CH); 3.85 (s, 3 H,  $\text{CO}_2\text{Me}$ ); 3.51 (s, 3 H,  $\text{CO}_2\text{Me}$ ).  $^1\text{H NMR}$  (acetone- $d_6$ ;  $\delta$ ): 7.4–6.6 (m, 20 H, Ph); 5.60 (s, 0.2 H,  $\text{CH}_2\text{Cl}_2$ ); 5.00 (s, 5 H,  $\text{C}_5\text{H}_5$ ); 4.19 (s, 1 H, CH); 3.83 (s, 3 H,  $\text{CO}_2\text{Me}$ ); 3.45 (s, 3 H,  $\text{CO}_2\text{Me}$ ). FAB MS: identical in observed peaks and intensities with those of **5a**. The instability of **5c** in solution prevented the isolation of crystals suitable for an X-ray study.

(b)  **$^1\text{H NMR}$  Study of the Conversion of 5a to 5b.** (i) Isomer **5a** in acetone- $d_6$  showed no appreciable change after 20 h in solution.

(ii) Isomer **5a** (30 mg, 0.041 mmol) in acetone- $d_6$  (3 mL), in the presence of silica (28–280 mesh; 225 mg), showed no appreciable change after 26 h in solution.

(iii) Isomer **5a** (10 mg, 0.014 mmol) was dissolved in  $\text{CH}_2\text{Cl}_2$  (10 mL), silica (TLC grade; 150 mg) was added, and the solvent was removed under reduced pressure. The sample was left in contact with air under normal lighting conditions. NMR samples were prepared by removing 15 mg of the silica sample and extracting with acetone- $d_6$  (0.5 mL). After 7 h approximately 50% conversion to **5c** was apparent; after 30 h, the conversion was 56%, and after 50 h, the conversion was 58%. Side reactions became prominent from 50 h onward. The only side reaction which could be correlated with the observed peaks was the conversion of **5a** to **5b**.

(c)  **$^1\text{H NMR}$  Study of the Conversion of 5b to 5a.** (i) Isomer **5b** in acetone- $d_6$  showed no appreciable change after 20 h in solution.

(ii) Isomer **5b** (10 mg, 0.014 mmol) was supported on silica (TLC grade; 125 mg) and sampled as above. After 48 h approximately 20% conversion to **5c** was indicated; at 14 days this had increased to 25% but with much side reaction (38%) and with only 37% of **5b** remaining. Of the side reactions only the conversion of **5b** to **5a** could be correlated with some of the observed peaks.

**Thermal Isomerization of Cyclobutenes 5a,b to the Butadienyl Complex  $\text{Ru}\{\text{C}=\text{C}(\text{CN})(\text{CO}_2\text{Me})\}\text{CPh}=\text{CH}(\text{CO}_2\text{Me})\}(\text{CO})(\text{PPh}_3)(\eta\text{-C}_5\text{H}_5)$  (**6**).** (a) **Conversion of 5a to 6.** Isomer **5a** (62 mg, 0.085 mmol) was dissolved in benzene (15 mL) and heated (oil bath, 94 °C) for 33 h. After the mixture was cooled, the solvent was removed under reduced pressure and the residue purified by TLC (petroleum ether/acetone/ $\text{CH}_2\text{Cl}_2$  7/3/1). The major yellow band ( $R_f$  0.42) crystallized ( $\text{CH}_2\text{Cl}_2/\text{EtOH}$ ) as yellow crystals of  $\text{Ru}\{\text{C}=\text{C}(\text{CN})(\text{CO}_2\text{Me})\}\text{CPh}=\text{CH}(\text{CO}_2\text{Me})\}(\text{CO})(\text{PPh}_3)(\eta\text{-C}_5\text{H}_5)$  (**6**; 45 mg, 0.062 mmol, 73%); mp 158–160 °C. Anal. Calcd for  $\text{C}_{39}\text{H}_{32}\text{NO}_5\text{PRu}$ : C, 64.46; H, 4.44; N, 1.91;  $M_r$ , 727. Found: C, 63.86; H, 4.51; N, 2.29;  $M_r$ , 727 (mass spectrometry). IR ( $\text{CH}_2\text{Cl}_2$ ;  $\text{cm}^{-1}$ ):  $\nu(\text{CN})$  2207 (w);  $\nu(\text{CO})$  1951 (s), 1725 (s), 1697 (sh).  $^1\text{H NMR}$  ( $\text{CDCl}_3$ ;  $\delta$ ): 7.6–7.1 (m, 20 H, Ph); 5.41 (s, 1 H, CH); 4.74 (s, 5 H,  $\text{C}_5\text{H}_5$ ); 3.58 (s, 3 H,  $\text{CO}_2\text{Me}$ ); 3.14 (s, 3 H,  $\text{CO}_2\text{Me}$ ). FAB MS ( $m/z$ ): 727\*,  $[\text{M}]^+$ , 25; 712\*,  $[\text{M} - \text{Me}]^+$ , 2; 698\*,  $[\text{M} - \text{CO}]^+$ , 9; 662\*,  $[\text{M} - (\text{C}_5\text{H}_5)]^+$ , 15; 634\*,  $[\text{M} - \text{CO} - (\text{C}_5\text{H}_5)]^+$ , 7; 457\*,  $[\text{Ru}(\text{CO})(\text{PPh}_3)(\text{C}_5\text{H}_5)]^+$ , 47; 429\*,  $[\text{Ru}(\text{PPh}_3)(\text{C}_5\text{H}_5)]^+$ , 100; 378\*,  $[\text{Ru}(\text{CO})(\text{PPh}_2)(\text{C}_5\text{H}_5)]^+$ , 11; 362\*,  $[\text{Ru}(\text{PPh}_3)]^+$ , 16; 350\*,  $[\text{Ru}(\text{PPh}_2)(\text{C}_5\text{H}_5)]^+$ , 21; 244,  $[\text{RuPh}(\text{C}_5\text{H}_5)]^+$ , 15; 167,  $[\text{Ru}(\text{C}_5\text{H}_5)]^+$ , 25. Of five minor/trace bands, two were identified: the first white band ( $R_f$  0.89) as  $\text{PPh}_3$  (by FAB MS and comparative spot TLC) and a second white band as unreacted **5a** (4 mg, 6%) (by  $^1\text{H NMR}$  and comparative spot TLC).

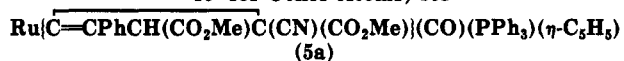
(b) **Conversion of 5b to 6.** Isomer **5b** (45 mg, 0.062 mmol) was dissolved in benzene (20 mL), and the solution was refluxed for 17 h. After cooling and removal of solvent under reduced pressure, the residue was purified by TLC (petroleum ether/ $\text{CH}_2\text{Cl}_2$ /acetone 4/2/1). A major yellow band ( $R_f$  0.53) was collected and crystallized ( $\text{CH}_2\text{Cl}_2$ /petroleum ether); this was identified by FAB MS and  $^1\text{H NMR}$  methods as **6** (13 mg, 0.018 mmol, 29%). Four white minor/trace bands were not characterized.

(c) **Direct Synthesis of 6.** A direct preparation of the butadienyl isomer that avoids unnecessary separation of the cyclobutenyl isomers is as follows. The crude reaction mixture obtained from the reaction between  $\text{Ru}(\text{C}_2\text{Ph})(\text{CO})(\text{PPh}_3)(\eta\text{-C}_5\text{H}_5)$  (220 mg, 0.39 mmol) and rjo (92 mg, 0.54 mmol) was evaporated to dryness. This residue was then precipitated from  $\text{CH}_2\text{Cl}_2/\text{MeOH}$  to give an off-white powder (200 mg, 0.28 mmol, 70%) consisting of a mixture of **5a** and **5b** (200 mg, 0.28 mmol). The powder was dissolved in benzene (30 mL), and the solution was refluxed for 16 h. After the mixture was cooled, the solvent was removed under reduced pressure and the residue purified by TLC (petroleum ether/ $\text{CH}_2\text{Cl}_2$ /acetone 4/2/1). A major yellow band ( $R_f$  0.53) was crystallized ( $\text{CH}_2\text{Cl}_2/\text{EtOH}$ ) to give yellow crystalline **6** (122 mg, 0.17 mmol, 60%). Two other bands were collected: a white band ( $R_f$  0.63) identified as **5a** (by  $^1\text{H NMR}$  and FAB MS), and a yellow band ( $R_f$  0.42) identified as **9** (by FAB MS and  $^1\text{H NMR}$ ).

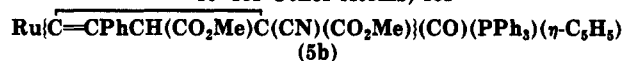
**Thermal Conversion of the Cyclobutenes 5a,b to  $\text{Ru}\{\eta^3\text{-CH}(\text{CO}_2\text{Me})\text{CPhC}=\text{C}(\text{CN})(\text{CO}_2\text{Me})\}(\text{CO})(\eta\text{-C}_5\text{H}_5)$  (**9**).** (a) **Conversion of 5a to 9.** Isomer **5a** (83 mg, 0.11 mmol) was heated in refluxing xylene (40 mL) for 24.5 h. After cooling and removal of solvent (vacuum, 30 °C) the residue was purified by TLC (petroleum ether/ $\text{CH}_2\text{Cl}_2$ /acetone 8/5/2). A major yellow band ( $R_f$  0.35) crystallized ( $\text{CH}_2\text{Cl}_2$ /petroleum ether) as large yellow crystals of  $\text{Ru}\{\eta^3\text{-CH}(\text{CO}_2\text{Me})\text{CPhC}=\text{C}(\text{CN})(\text{CO}_2\text{Me})\}(\text{CO})(\eta\text{-C}_5\text{H}_5)\cdot\text{CH}_2\text{Cl}_2$  (**9**; 29 mg, 0.06 mmol, 57%), mp 111–112 °C. Anal. Calcd for  $\text{C}_{21}\text{H}_{17}\text{NO}_5\text{Ru}\cdot\text{CH}_2\text{Cl}_2$ : C, 48.09; H, 3.48; N, 2.55;  $M_r$ , 465 (unsolvated). Found: C, 48.18; H, 3.46; N, 2.64;  $M_r$ , 465 (mass spectrometry). IR ( $\text{CH}_2\text{Cl}_2$ ;  $\text{cm}^{-1}$ ):  $\nu(\text{CN})$  2220 (w);  $\nu(\text{CO})$  2014 (vs) 1736 (sh), 1715 (s), 1665 (w).  $^1\text{H NMR}$  ( $\text{CDCl}_3$ ;  $\delta$ ): 7.3–7.2 (m, 5 H, Ph); 5.30 (s, 2 H,  $\text{CH}_2\text{Cl}_2$ ); 5.09 (s, 1 H, CH); 5.04 (s, 5 H,  $\text{C}_5\text{H}_5$ ); 3.66 (s, 3 H,  $\text{CO}_2\text{Me}$ ); 3.55 (s, 3 H,  $\text{CO}_2\text{Me}$ ). FAB MS ( $m/z$ ): 465,  $[\text{M}]^+$ , 25; 437\*,  $[\text{M} - \text{CO}]^+$ , 100; 422,  $[\text{M} - \text{Me}]^+$ , 38; 378\*,  $[\text{M} - \text{CO} - \text{CO}_2\text{Me}]^+$ , 52; 320,  $[\text{M} - \text{CO} - 2\text{CO}_2\text{Me}]^+$ , 13; 167\*,  $[\text{Ru}(\text{C}_5\text{H}_5)]^+$ , 27. Higher mass ions are also formed with relative abundance <5% ( $m/z$ ): 930\*,  $[\text{M}_2]^+$ ; 902\*,  $[\text{M}_2 - \text{CO}]^+$ ;

Table II. Crystal Data and Refinement Details for Complexes 5a,b, 6, and 9

	5a	5b	6	9
formula	C <sub>39</sub> H <sub>32</sub> NO <sub>5</sub> PRu	C <sub>39</sub> H <sub>32</sub> NO <sub>5</sub> PRu	C <sub>40</sub> H <sub>34</sub> Cl <sub>2</sub> NO <sub>5</sub> PRu	C <sub>21</sub> H <sub>17</sub> NO <sub>5</sub> Ru
<i>M<sub>r</sub></i>	726.7	726.7	811.6	464.4
cryst syst	monoclinic	orthorhombic	triclinic	monoclinic
space group	<i>P</i> 2 <sub>1</sub> / <i>c</i> (C <sub>2h</sub> <sup>5</sup> , No. 14)	<i>Pna</i> 2 <sub>1</sub> (C <sub>2h</sub> <sup>6</sup> , No. 33)	<i>P</i> 1̄ (C <sub>1</sub> <sup>1</sup> , No. 2)	<i>P</i> 2 <sub>1</sub> / <i>n</i> (variant C <sub>2h</sub> <sup>5</sup> , No. 14)
<i>a</i> , Å	14.719 (13)	18.188 (7)	9.227 (5)	9.018 (3)
<i>b</i> , Å	11.851 (6)	18.059 (4)	13.069 (9)	12.244 (2)
<i>c</i> , Å	18.572 (13)	10.349 (5)	15.860 (8)	18.060 (4)
$\alpha$ , deg	90	90	98.44 (3)	90
$\beta$ , deg	91.29 (4)	90	92.17 (4)	104.56 (2)
$\gamma$ , deg	90	90	103.91 (3)	90
<i>V</i> , Å <sup>3</sup>	3238.8	3399.2	1831.0	1929.9
<i>Z</i>	4	4	2	4
<i>D<sub>c</sub></i> , g cm <sup>-3</sup>	1.490	1.420	1.472	1.598
$\mu$ , cm <sup>-1</sup>	5.34	5.07	6.12	7.96
<i>F</i> (000)	1488	1488	828	936
$\vartheta$ range	1.3–27.0	1.3–21.0	1.5–23.0	2.0–25.0
no. of unique rflns	3448	1958	3813	3385
criterion of observability	2.5	2.0	2.0	3.0
no. of obsd rflns	3115	1813	3588	2813
<i>R</i>	0.040	0.043	0.050	0.034
<i>k</i>	5.04	2.47	1.0	1.0
<i>g</i>	0.0001	0.0005		0.0012
<i>R<sub>w</sub></i>	0.050	0.050	0.059	0.038

Table III. Fractional Atomic Coordinates ( $\times 10^5$  for Ru,  $\times 10^4$  for Other Atoms) for

atom	<i>x</i>	<i>y</i>	<i>z</i>
Ru	17517 (3)	22663 (3)	31838 (2)
P(1)	2584 (1)	693 (1)	3499 (1)
O(1)	2359 (3)	5869 (3)	4594 (2)
O(2)	2303 (2)	5710 (3)	5791 (2)
O(3)	-481 (2)	3273 (4)	4558 (2)
O(4)	514 (2)	2396 (3)	5279 (2)
O(5)	73 (2)	1037 (3)	3609 (2)
N(1)	405 (4)	5402 (4)	3700 (3)
C(1)	1327 (3)	2547 (3)	2023 (2)
C(2)	2265 (3)	2268 (3)	2049 (2)
C(3)	2732 (3)	3127 (3)	2440 (2)
C(4)	2083 (3)	3938 (3)	2657 (2)
C(5)	1214 (3)	3579 (3)	2399 (2)
C(6)	1848 (3)	3076 (4)	4165 (3)
C(7)	2454 (3)	3363 (4)	4695 (3)
C(8)	3420 (2)	3204 (3)	4888 (2)
C(9)	3668 (2)	2567 (3)	5492 (2)
C(10)	4580 (2)	2491 (3)	5709 (2)
C(11)	5243 (2)	3052 (3)	5320 (2)
C(12)	4994 (2)	3689 (3)	4716 (2)
C(13)	4083 (2)	3765 (3)	4500 (2)
C(14)	1822 (3)	4138 (4)	5111 (3)
C(15)	2158 (3)	5333 (4)	5125 (3)
C(16)	2605 (4)	6871 (5)	5855 (4)
C(17)	1096 (3)	3812 (4)	4518 (3)
C(18)	275 (4)	3154 (5)	4783 (3)
C(19)	-226 (4)	1718 (5)	5536 (4)
C(20)	726 (4)	4733 (5)	4063 (3)
C(21)	724 (4)	1526 (4)	3458 (3)
C(22)	2796 (2)	333 (3)	4449 (2)
C(23)	3617 (2)	-119 (3)	4705 (2)
C(24)	3713 (2)	-441 (3)	5425 (2)
C(25)	2989 (2)	-311 (3)	5890 (2)
C(26)	2168 (2)	141 (3)	5634 (2)
C(27)	2072 (2)	463 (3)	4914 (2)
C(28)	2103 (2)	-643 (2)	3152 (2)
C(29)	1516 (2)	-627 (2)	2552 (2)
C(30)	1191 (2)	-1638 (2)	2259 (2)
C(31)	1455 (2)	-2664 (2)	2567 (2)
C(32)	2042 (2)	-2680 (2)	3167 (2)
C(33)	2366 (2)	-1669 (2)	3459 (2)
C(34)	3721 (2)	689 (3)	3106 (2)
C(35)	4341 (2)	1516 (3)	3328 (2)
C(36)	5177 (2)	1607 (3)	2993 (2)
C(37)	5392 (2)	872 (3)	2436 (2)
C(38)	4772 (2)	45 (3)	2214 (2)
C(39)	3937 (2)	-46 (3)	2549 (2)

Table IV. Fractional Atomic Coordinates ( $\times 10^5$  for Ru,  $\times 10^4$  for Other Atoms) for

atom	<i>x</i>	<i>y</i>	<i>z</i>
Ru	20031 (3)	7181 (3)	25000 (-)
P(1)	3178 (1)	1140 (1)	2867 (2)
O(1)	510 (4)	1859 (4)	7714 (14)
O(2)	1673 (4)	2022 (4)	7238 (9)
O(3)	74 (5)	328 (8)	4381 (10)
O(4)	-135 (5)	1402 (4)	3367 (10)
O(5)	1496 (4)	2188 (4)	1511 (8)
N(1)	918 (5)	2769 (5)	4428 (12)
C(1)	1755 (5)	75 (4)	709 (7)
C(2)	1157 (5)	-10 (4)	1578 (7)
C(3)	1423 (5)	-373 (4)	2702 (7)
C(4)	2185 (5)	-512 (4)	2527 (7)
C(5)	2390 (5)	-235 (4)	1296 (7)
C(6)	1628 (5)	951 (5)	4369 (11)
C(7)	1736 (5)	742 (4)	5600 (10)
C(8)	2260 (4)	242 (3)	6284 (8)
C(9)	2752 (4)	540 (3)	7178 (8)
C(10)	3233 (4)	76 (3)	7846 (8)
C(11)	3224 (4)	-685 (3)	7618 (8)
C(12)	2732 (4)	-982 (3)	6723 (8)
C(13)	2250 (4)	-519 (3)	6056 (8)
C(14)	1047 (5)	1079 (5)	6157 (11)
C(15)	1040 (7)	1667 (7)	7163 (13)
C(16)	1659 (11)	2665 (9)	8073 (19)
C(17)	897 (5)	1339 (5)	4736 (10)
C(18)	233 (6)	957 (7)	4167 (13)
C(19)	-781 (7)	1060 (9)	2761 (23)
C(20)	889 (5)	2153 (6)	4549 (11)
C(21)	1694 (5)	1615 (6)	1953 (10)
C(22)	3365 (3)	1769 (3)	4214 (7)
C(23)	4012 (3)	1738 (3)	4935 (7)
C(24)	4161 (3)	2283 (3)	5854 (7)
C(25)	3662 (3)	2859 (3)	6051 (7)
C(26)	3015 (3)	2890 (3)	5330 (7)
C(27)	2867 (3)	2345 (3)	4411 (7)
C(28)	3835 (3)	374 (3)	3066 (6)
C(29)	3845 (3)	-28 (3)	4215 (6)
C(30)	4315 (3)	-634 (3)	4346 (6)
C(31)	4775 (3)	-837 (3)	3328 (6)
C(32)	4765 (3)	-434 (3)	2178 (6)
C(33)	4295 (3)	172 (3)	2047 (6)
C(34)	3599 (3)	1666 (4)	1546 (5)
C(35)	4273 (3)	2020 (4)	1728 (5)
C(36)	4585 (3)	2429 (4)	726 (5)
C(37)	4224 (3)	2484 (4)	-459 (5)
C(38)	3550 (3)	2130 (4)	-641 (5)
C(39)	3237 (3)	1721 (4)	361 (5)



**Table V. Fractional Atomic Coordinates ( $\times 10^5$  for Ru,  $\times 10^4$  for Other Atoms) for  $\text{Ru}[\text{C}(\equiv\text{C}(\text{CN})(\text{CO}_2\text{Me})]\text{CPh}=\text{CH}(\text{CO}_2\text{Me})(\text{CO})(\text{PPh}_3)(\eta\text{-C}_5\text{H}_5)$  (6)**

atom	x	y	z
Ru(1)	50086 (6)	78587 (4)	75512 (3)
P(1)	2832 (2)	6495 (1)	7328 (1)
O(1)	655 (6)	8792 (4)	7078 (3)
O(2)	480 (5)	9327 (5)	5812 (3)
O(3)	2897 (7)	11084 (4)	8237 (4)
O(4)	1562 (6)	10203 (4)	9173 (3)
O(5)	5360 (5)	7956 (4)	5693 (3)
N(1)	3485 (7)	8676 (5)	9920 (4)
C(1)	6605 (5)	8654 (4)	8718 (3)
C(2)	7451 (5)	8544 (4)	8006 (3)
C(3)	7219 (6)	7448 (4)	7696 (3)
C(4)	6230 (6)	6880 (4)	8217 (4)
C(5)	5851 (5)	7625 (4)	8849 (3)
C(6)	3877 (6)	9085 (5)	7766 (4)
C(7)	3943 (7)	9723 (5)	7073 (4)
C(8)	5447 (3)	10425 (4)	6992 (3)
C(9)	5927 (6)	10632 (5)	6202 (3)
C(10)	7310 (7)	11320 (5)	6144 (4)
C(11)	8219 (6)	11805 (5)	6864 (4)
C(12)	7761 (6)	11609 (5)	7648 (4)
C(13)	6381 (6)	10923 (4)	7717 (3)
C(14)	2830 (8)	9707 (6)	6494 (5)
C(15)	1263 (8)	9226 (6)	6507 (5)
C(16)	-1100 (10)	8943 (10)	5751 (7)
C(17)	3329 (7)	9426 (6)	8513 (5)
C(18)	2624 (8)	10336 (7)	8614 (5)
C(19)	738 (11)	11007 (8)	9284 (6)
C(20)	3379 (7)	8959 (6)	9279 (5)
C(21)	5126 (6)	7930 (5)	6409 (5)
C(22)	3185 (5)	5169 (3)	7005 (3)
C(23)	2345 (5)	4246 (4)	7254 (3)
C(24)	2592 (6)	3258 (3)	6939 (4)
C(25)	3668 (6)	3181 (4)	6381 (4)
C(26)	4506 (5)	4084 (4)	6130 (3)
C(27)	4271 (5)	5077 (3)	6439 (3)
C(28)	1862 (5)	6433 (4)	8299 (3)
C(29)	2277 (5)	5935 (4)	8949 (3)
C(30)	1555 (6)	5949 (4)	9702 (3)
C(31)	424 (5)	6456 (4)	9813 (3)
C(32)	3 (5)	6952 (4)	9177 (3)
C(33)	714 (5)	6944 (4)	8421 (3)
C(34)	1323 (5)	6373 (4)	6509 (3)
C(35)	-75 (5)	5708 (4)	6569 (3)
C(36)	-1209 (4)	5552 (4)	5927 (4)
C(37)	-963 (5)	6051 (4)	5227 (3)
C(38)	410 (6)	6709 (4)	5159 (3)
C(39)	1555 (5)	6873 (4)	5796 (3)
C(40)	5522 (16)	3215 (8)	8585 (8)
Cl(1)	4434 (5)	3840 (3)	9247 (2)
Cl(2)	6867 (5)	4146 (2)	8145 (2)

630\*,  $[\text{M} + \text{Ru}(\text{C}_5\text{H}_5)]^+$ ; 602\*,  $[630 - \text{CO}]^+$ . Of the remaining four minor/trace bands, only two were identified: a white band ( $R_f$  0.73) as  $\text{PPh}_3$  (FAB MS, spot TLC) and a yellow band ( $R_f$  0.46) as **6** ( $^1\text{H}$  NMR, FAB MS).

(b) **Conversion of 5b to 9.** Isomer **5b** (58 mg, 0.08 mmol) was dissolved in toluene (10 mL), and the solution was heated at reflux point for 29 h. After the mixture was cooled, the solvent was removed under reduced pressure and the residue purified by TLC (petroleum ether/acetone/ $\text{CH}_2\text{Cl}_2$  7/3/1). A major yellow band ( $R_f$  0.44) was identified (by IR,  $^1\text{H}$  NMR, and FAB MS) as **9** (14 mg, 0.03 mmol, 38%). Of the five minor/trace bands, only one was identified, a white band ( $R_f$  0.86) as  $\text{PPh}_3$  (by FAB MS and comparative spot TLC).

### Crystallography

**Single-Crystal X-ray Diffraction Studies of 5a,b, 6, and 9.** Intensity data for **5a,b** and **6** were measured at room temperature on an Enraf-Nonius CAD4F diffractometer fitted with  $\text{Mo K}\alpha$  (graphite monochromator) radiation ( $\lambda = 0.7107 \text{ \AA}$ ). Data for **9** were obtained at 193 K on a Nicolet P3 diffractometer also fitted with  $\text{Mo K}\alpha$  radiation. The monitoring of intensity

**Table VI. Fractional Atomic Coordinates ( $\times 10^5$  for Ru,  $\times 10^4$  for Other Atoms) for  $\text{Ru}[\eta^3\text{-C}(\equiv\text{C}(\text{CN})(\text{CO}_2\text{Me})]\text{CPh}=\text{CH}(\text{CO}_2\text{Me})(\text{CO})(\eta\text{-C}_5\text{H}_5)$  (9)**

atom	x	y	z
Ru	68192 (3)	32458 (2)	86179 (2)
O(1)	7595 (3)	408 (2)	8275 (2)
O(2)	9523 (3)	874 (2)	9282 (2)
O(3)	3321 (4)	59 (3)	6781 (2)
O(4)	3689 (3)	106 (2)	8052 (2)
O(5)	8488 (4)	2587 (3)	7433 (2)
N(1)	4249 (5)	2477 (3)	6118 (2)
C(1)	6730 (4)	5038 (3)	8400 (1)
C(2)	8202 (4)	4774 (3)	8868 (1)
C(3)	8009 (4)	4354 (3)	9571 (1)
C(4)	6418 (4)	4358 (3)	9537 (1)
C(5)	5628 (4)	4780 (3)	8813 (1)
C(6)	5221 (4)	2114 (3)	8103 (2)
C(7)	5586 (4)	1856 (3)	8896 (2)
C(8)	4447 (3)	2002 (2)	9361 (1)
C(9)	3171 (3)	2676 (2)	9113 (1)
C(10)	2138 (3)	2811 (2)	9567 (1)
C(11)	2382 (3)	2273 (2)	10268 (1)
C(12)	3658 (3)	1599 (2)	10516 (1)
C(13)	4691 (3)	1464 (2)	10063 (1)
C(14)	7179 (4)	1655 (3)	9224 (2)
C(15)	8061 (5)	917 (3)	8858 (2)
C(16)	10554 (5)	204 (4)	8976 (3)
C(17)	4448 (4)	1636 (3)	7449 (2)
C(18)	3760 (4)	529 (3)	7384 (2)
C(19)	3046 (5)	-978 (4)	8009 (3)
C(20)	4357 (4)	2127 (3)	6712 (2)
C(21)	7849 (5)	2810 (4)	7886 (2)

standards during each data collection indicated that a 27% decrease in the net intensities for **6** had occurred, and the data set for this compound was corrected accordingly; no significant decomposition of **5a,b** or **9** occurred during their respective data collections. The data sets were corrected for Lorentz and polarization effects, and absorption corrections were also applied using a Gaussian procedure<sup>18</sup> for **5a,b** and **6** and the  $\phi$ -scan technique for **9**. Relevant crystal data are listed in Table II.

Each of the structures was solved by the Patterson technique, and refinement of the structures was achieved by a full-matrix least-squares procedure for **5a,b** and **9** with SHELX76,<sup>19</sup> while for **6** the program RAELS<sup>20</sup> was employed. Anisotropic thermal parameters were introduced for the Ru, N, O, P, and cyclopentadienyl carbon atoms in **5a**, the Ru, N, O, P, and methyl carbon atoms in **5b**, and all non-H atoms in **6** and **9**. Phenyl groups were refined as hexagonal rigid groups in the structures of **5a,b** and **9**; cyclopentadienyl groups were refined as pentagonal rigid groups in all four refinements. Hydrogen atoms were included in their calculated positions for each model. A weighting scheme of the form  $w = k[\sigma^2(F) + gF^2]^{-1}$  was included in the refinements of **5a,b** and **9**; for **6** a weighting scheme of the form  $[\sigma^2(I) + 0.04I^2]^{1/2}$  was applied. Final refinement details for the four structures are given in Table II. The absolute configuration of **5b** could not be determined, as there were no significant differences in Friedel pairs included in the data set.

Scattering factors for neutral Ru (corrected for  $f'$  and  $f''$ ) were from ref 21, while those for the remaining atoms were the ones incorporated in SHELX76<sup>19</sup> or RAELS.<sup>20</sup> The final fractional atomic coordinates are listed in Tables III–VI, and selected interatomic parameters are given in Table I. The numbering schemes employed are shown in Figures 1–4, which were drawn with 15% probability ellipsoids by ORTEP.<sup>22</sup>

(19) Sheldrick, G. M. SHELX76, Programme for Crystal Structure Determination; University of Cambridge, Cambridge, U.K., 1976.

(20) (a) Rae, A. D. RAELS, A Comprehensive Constrained Least-Squares Refinement Program; University of New South Wales: Kensington, Australia, 1984. (b) Rae, A. D. *Acta Crystallogr., Sect. A* 1975, 31, 560.

(21) Ibers, J. A., Hamilton, W. C., Eds. *International Tables for X-ray Crystallography*; Kynoch: Birmingham, U.K., 1974; Vol. 4, pp 99, 142.

(22) Johnson, C. K. ORTEP, Report ORNL-3794; Oak Ridge National Laboratory: Oak Ridge, TN, 1976.

**Acknowledgment.** We thank the Australian Research Council for financial support of this work. We thank Professor W. R. Jackson (Monash University) for a generous gift of the olefin **1j**. We are grateful to Drs. E. Horn (**5a,b**), D. Craig (**6**), and W. T. Robinson (**9**) for collection

(23) The absolute configurations at ruthenium in **5a,b** can be specified using the Baird-Sloan modifications of the Cahn-Ingold-Prelog priority rules.<sup>24</sup> Thus, the two enantiomers of **5a** in the crystal have *R* and *S* configurations at Ru (*R* illustrated in Figure 1). Spontaneous resolution of **5b** occurred on crystallization, the crystal used for the X-ray study containing only the *R* enantiomer.

(24) Stanley, K.; Baird, M. C. *J. Am. Chem. Soc.* 1975, 97, 6598.

of intensity data for the indicated complexes. M.J.L. was the holder of a Commonwealth Post-Graduate Research Award.

**Registry No.** **5a**, 138630-25-8; **5b**, 138749-87-8; **5c**, 138749-88-9; **6**, 138630-27-0; **9**, 138630-28-1; C(CN)(CO<sub>2</sub>Me)=CH(CO<sub>2</sub>Me), 54797-29-4; Ru(C<sub>2</sub>Ph)(CO)(PPh<sub>3</sub>)( $\eta$ -C<sub>5</sub>H<sub>5</sub>), 75592-69-7.

**Supplementary Material Available:** Tables of fractional atomic coordinates, anisotropic thermal parameters, and bond distances and angles for the four structures (14 pages); tables of structure factor amplitudes (59 pages). Ordering information is given on any current masthead page.

## Cyclopalladation of *N*-Mesitylbenzylideneamines. Aromatic versus Aliphatic C-H Activation

Joan Albert, Rosa Maria Ceder, Montserrat Gómez, Jaume Granell, and Joaquim Sales\*

Departament de Química Inorgànica, Universitat de Barcelona, Diagonal, 647, 08028 Barcelona, Spain

Received September 11, 1991

The action of Pd(AcO)<sub>2</sub> on the imines 2,4,6-(CH<sub>3</sub>)<sub>3</sub>C<sub>6</sub>H<sub>2</sub>CH=N(CH<sub>2</sub>)<sub>n</sub>-2'-RC<sub>6</sub>H<sub>4</sub> (R = H, *n* = 0-2 (**1a-c**); R = CH<sub>3</sub>, *n* = 1 (**1d**)), in refluxing acetic acid, affords six-membered endo metallacycles possessing an aliphatic carbon-metal bond, in preference to four-, five-, or six-membered exo metallacycles with an aromatic carbon-metal bond. The five-membered exo metallacycles can be obtained by working under milder conditions and isomerize to the more stable six-membered endo metallacycles in refluxing acetic acid. The action of Pd(AcO)<sub>2</sub> on the imines 2-CH<sub>3</sub>-3-R<sup>1</sup>-4-R<sup>2</sup>C<sub>6</sub>H<sub>2</sub>CH=NC<sub>6</sub>H<sub>5</sub> (R<sup>1</sup> = H, R<sup>2</sup> = CH<sub>3</sub> (**1f**); R<sup>1</sup> = CH<sub>3</sub>, R<sup>2</sup> = CH<sub>3</sub>O (**1g**)) affords the five-membered endo metallacycles with an aromatic carbon-metal bond, but with the imine 2,5-(CH<sub>3</sub>)<sub>2</sub>C<sub>6</sub>H<sub>3</sub>CH=NC<sub>6</sub>H<sub>5</sub> (**1e**) the methyl group at carbon 5 prevents the metalation of the ortho carbon atom and the endo six-membered metallacycle with an aliphatic carbon-metal bond is formed. The reasons for the preference to form endo compounds and the high stability of six-membered derivatives containing Pd-C benzylic bonds are discussed.

### Introduction

The question of aromatic versus aliphatic C-H bond activation has aroused considerable interest over the last few years. In intermolecular processes where an oxidative addition of C-H bonds occurs, it has been observed that there are many more examples of aromatic than aliphatic or benzylic C-H activations. Although the benzylic and allylic C-H bonds are weaker than the aromatic ones, the greater bond strength of the M-C<sub>aryl</sub> over the M-C<sub>alkyl</sub> or M-C<sub>benzyl</sub> bonds has been proposed as the explanation.<sup>1</sup>

It is generally accepted that there may be substantial similarities between intermolecular and intramolecular activations of C-H bonds; thus, the study of cyclo-metalation reactions may give valuable insight into intermolecular C-H activations.<sup>2</sup>

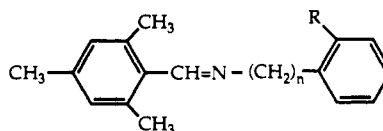
Cyclopalladation reactions of *N*-donor ligands have been extensively studied, but the factors that control the process are not thoroughly understood. In general, an intramolecular electrophilic attack of the metal at the carbon atom, a strong tendency to form five-membered rings, and preferential activation of aromatic over aliphatic C-H bonds are widely accepted.<sup>3</sup> Although electrophilic dis-

(1) (a) Hill, C. L. *Activation and Functionalization of Alkanes*; Wiley: New York, 1989. (b) Jones, W. D.; Feher, F. J. *Acc. Chem. Res.* 1989, 22, 91. (c) Jones, W. D.; Feher, F. J. *J. Am. Chem. Soc.* 1984, 107, 620. (d) Crabtree, R. H. *Chem. Rev.* 1985, 85, 245. (e) Halpern, J. *Inorg. Chim. Acta* 1985, 100, 41.

(2) (a) Lavin, M.; Holt, E. M.; Crabtree, R. H. *Organometallics* 1989, 8, 99. (b) Ryabov, A. D. *Chem. Rev.* 1990, 90, 403.

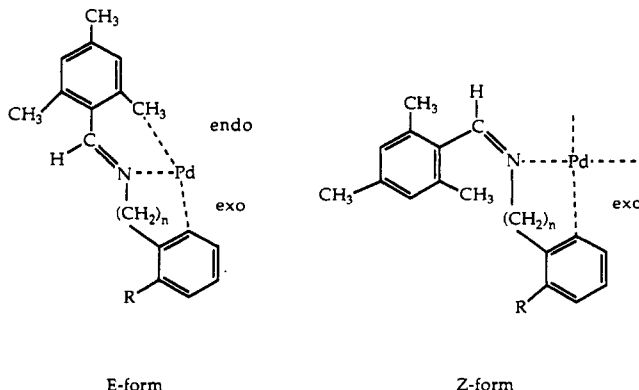
(3) (a) Brice, M. I. *Angew. Chem., Int. Ed. Engl.* 1977, 10, 73. (b) Omae, I. *Chem. Rev.* 1979, 79, 287. (c) Newkome, G. R.; Puckett, W. E.; Gupta, V. K.; Kiefer, G. E. *Chem. Rev.* 1986, 86, 451. (d) Omae, I. *Coord. Chem. Rev.* 1988, 83, 137. (e) Dunina, V. V.; Zalevskaia, O. A.; Potatov, V. M. *Russ. Chem. Rev.* 1988, 57, 250.

Chart I



- 1a** (*n*=0, R=H)  
**1b** (*n*=1, R=H)  
**1c** (*n*=2, R=H)  
**1d** (*n*=1, R=CH<sub>3</sub>)

Chart II



sociation of C-H bonds is not as severely limited as is oxidative addition by thermodynamic constraints associated with the weakness of M-H and M-C bonds and, for example, the stabilization of the leaving group H<sup>+</sup> is important in the thermodynamic driving force of the process,